

Probing the Origin of the Star Formation Excess Discovered by JWST through Gamma-Ray Bursts

TATSUYA MATSUMOTO,^{1,2} YUICHI HARIKANE,³ KEIICHI MAEDA,¹ AND KUNIHITO IOKA⁴

¹*Department of Astronomy, Kyoto University, Kitashirakawa-Oiwake-cho, Sakyo-ku, Kyoto, 606-8502, Japan*

²*Hakubi Center, Kyoto University, Yoshida-honmachi, Sakyo-ku, Kyoto, 606-8501, Japan*

³*Institute for Cosmic Ray Research, The University of Tokyo, 5-1-5 Kashiwanoha, Kashiwa, Chiba 277-8582, Japan*

⁴*Center for Gravitational Physics and Quantum Information, Yukawa Institute for Theoretical Physics, Kyoto University, Kyoto 606-8502, Japan*

ABSTRACT

The recent observations by the James Webb Space Telescope (JWST) have revealed a larger number of bright galaxies at $z \gtrsim 10$ than was expected. The origin of this excess is still under debate, although several possibilities have been presented. We propose that gamma-ray bursts (GRBs) are a powerful probe to explore the origin of the excess and, hence, the star and galaxy formation histories in the early universe. Focusing on the recently launched mission, Einstein Probe (EP), we find that EP can detect several GRBs annually at $z \gtrsim 10$, assuming the GRB formation rate calibrated by events at $z \lesssim 6$ can be extrapolated. Interestingly, depending on the excess scenarios, the GRB event rate may also show an excess at $z \simeq 10$, and its detection will help to discriminate between the scenarios that are otherwise difficult to distinguish. Additionally, we discuss that the puzzling, red-color, compact galaxies discovered by JWST, the so-called “little red dots”, could host dark GRBs if they are dust-obscured star forming galaxies. We are eager for unbiased follow-up of GRBs and encourage future missions such as HiZ-GUNDAM to explore the early universe.

Keywords: XXX

1. INTRODUCTION

Gamma-ray bursts (GRBs) are among the most luminous explosions in the universe, allowing them to be detected from large distances (Lamb & Reichart 2000; Ciardi & Loeb 2000; Gou et al. 2004). This characteristic makes GRBs invaluable as probe of the distant universe. In particular, long GRBs, which have a nominal duration of longer than 2 s (Kouveliotou et al. 1993), are produced by the collapse of massive stars (e.g., Woosley 1993; MacFadyen & Woosley 1999) and thus serve as powerful tools for investigating star formation processes throughout cosmic history (Totani 1997; Wijers et al. 1998; Krumholz et al. 1998; Mao & Mo 1998; Blain & Natarajan 2000; Porciani & Madau 2001). Actually, the detection of high- z GRBs at $z \gtrsim 6$ by *Swift* (see, Salvaterra 2015, for a review) has prompted active researches into the potential of GRBs to explore the history of cosmic star formation (Price et al. 2006; Daigne et al. 2006; Le & Dermer 2007; Guetta & Piran 2007; Chary et al. 2007; Kistler et al. 2008; Li 2008; Yüksel et al. 2008; Kistler et al. 2009; Wang & Dai 2009; Qin et al. 2010; Wanderman & Piran 2010; Ishida et al. 2011; Robertson & Ellis 2012; Salvaterra et al. 2012; Wang 2013), reionization (Kawai et al. 2006; Totani et al. 2006; Gallerani et al. 2008; McQuinn et al. 2008; Greiner et al. 2009; Patel et al. 2010; Chornock et al. 2013; Totani

et al. 2014; Hartoog et al. 2015; Fausey et al. 2024, see also Miralda-Escudé 1998), and the first generation of stars (Bromm & Loeb 2006; Mészáros & Rees 2010; de Souza et al. 2011; Suwa & Ioka 2011; Toma et al. 2011; Nagakura et al. 2012; Nakauchi et al. 2012; Kashiyama et al. 2013; Matsumoto et al. 2015, 2016; Kinugawa et al. 2019).

Recently, significant progress has been made in observations of the high- z universe with the advent of the James Webb Space Telescope (JWST). JWST not only broke the record for the most distant galaxy observed but also revealed that there are more abundant bright galaxies than previously expected (e.g., Finkelstein et al. 2022, 2023, 2024; Naidu et al. 2022; Adams et al. 2023, 2024; Bouwens et al. 2023a,b; Castellano et al. 2023; Donnan et al. 2023b,a, 2024; Harikane et al. 2023a, 2024a,b; Pérez-González et al. 2023; McLeod et al. 2024; Robertson et al. 2024). Various ideas have been proposed to explain this “JWST excess” in the UV luminosity function, such as active star formation (Dekel et al. 2023; Li et al. 2023), top-heavy initial mass function (Inayoshi et al. 2022; Steinhardt et al. 2023), and even a flaw in the cosmological model (Parashari & Laha 2023); however, the cause remains unclear, and it has become one of the topics of active debate (see discussions in Harikane et al. 2023a, 2024a,b).

In this letter, we explore the detectability of high- z GRBs and their potential to elucidate the origin of the excess discovered by JWST. In particular, we focus on the observational prospect of the *Einstein Probe* (EP, Yuan et al. 2022)¹, which was launched in January 2024 and has begun its observations. EP has a sensitive soft X-ray detector Wide X-ray Telescope (WXT), being advantageous for observing high- z GRBs. In fact, a GRB at $z = 4.859$ was already detected (Gillanders et al. 2024; Liu et al. 2024; Levan et al. 2024; Ricci et al. 2024). We find that depending on potential origins of the JWST excess, the GRB formation rate can have different behaviors around $z \gtrsim 10$, and its detection by EP or future GRB missions will clarify the cause of the JWST excess.

The paper is organized as follows. In Sec. 2 we describe the method to calculate the event rate of GRBs. In Sec. 3, various possibilities on the GRB event rates at $z \gtrsim 10$ are discussed along with the origin of the JWST excess. We present our results in Sec. 4, and summarize our findings in Sec. 5. Throughout this Letter, we assume Λ CDM cosmology and use the cosmological parameters of $H_0 = 67.4 \text{ km s}^{-1} \text{ Mpc}^{-1}$, $\Omega_m = 0.315$, and $\Omega_\Lambda = 0.685$ (Planck Collaboration et al. 2020).

2. EVENT RATE OF HIGH-Z GRBS

The number of GRBs detected by a detector during an observation time Δt_{obs} and for a redshift range of $(z, z + dz)$ is calculated by (e.g., Bromm & Loeb 2006; de Souza et al. 2011)

$$\frac{dN_{\text{GRB}}}{dz} = \Psi_{\text{GRB}}^{\text{obs}} \frac{\Delta t_{\text{obs}}}{1+z} \frac{dV}{dz}, \quad (1)$$

where $\Psi_{\text{GRB}}^{\text{obs}}$ is the observed comoving event rate of GRBs, that is the number of observable GRBs per comoving volume and time, discussed in the next paragraph, and the cosmological volume element is given by

$$\frac{dV}{dz} = \frac{4\pi c d_L^2}{1+z} \left| \frac{dt}{dz} \right| = \frac{4\pi c d_L^2}{(1+z)^2 H_0 \sqrt{\Omega_m (1+z)^3 + \Omega_\Lambda}}. \quad (2)$$

Here c and d_L are the speed of light and the luminosity distance, respectively.

The comoving event rate of GRBs observed by the detector covering a solid angle Ω in the sky is given by

$$\Psi_{\text{GRB}}^{\text{obs}}(z) = \frac{\Omega}{4\pi} \eta_{\text{beam}} \Psi_{\text{GRB}}(z) \int_{L_{\text{min}}(z)}^{\infty} \frac{dn}{dL} dL, \quad (3)$$

where η_{beam} is the beaming factor giving a fraction of on-axis events, $\Psi_{\text{GRB}}(z)$ is the intrinsic comoving GRB formation rate, $L_{\text{min}}(z)$ is the minimal GRB luminosity

to trigger the detector, and dn/dL is the normalized luminosity function (LF, $\int \frac{dn}{dL} dL = 1$). In this Letter we call an isotropic equivalent gamma-ray luminosity as a luminosity for simplicity. For a jet with a half-opening angle θ_j , the beaming factor is given by

$$\eta_{\text{beam}} = 1 - \cos \theta_j \simeq \frac{\theta_j^2}{2} \simeq 0.005 \left(\frac{\theta_j}{0.1} \right)^2, \quad (4)$$

where $\theta_j = 0.1$ is an observationally motivated value (e.g., Frail et al. 2001; Goldstein et al. 2016). Our results will linearly depend on the beaming factor.

The minimal luminosity in Eq. (3) is calculated by equating a flux of a prompt GRB emission with the detector's sensitivity. To obtain the former one, we assume that the prompt emission has the Band spectrum (Band et al. 1993):

$$N(E) = A \begin{cases} \left(\frac{E}{100} \right)^\beta \left(\frac{(\alpha-\beta)E_0}{100e} \right)^{\alpha-\beta} & : E < (\alpha-\beta)E_0, \\ \left(\frac{E}{100} \right)^\alpha \exp\left(-\frac{E}{E_0}\right) & : (\alpha-\beta)E_0 < E, \end{cases} \quad (5)$$

where A and e are a normalization and the Napier's constant, respectively. The photon energy is measured in a unit of keV. We fix the low and high energy power-law indices to typical values of $\alpha = -1$ and $\beta = -2.3$ (Preece et al. 2000; Kaneko et al. 2006), respectively. E_0 is the cut-off energy, which is related to the peak energy in the energy spectrum, $E^2 N(E)$, as $E_p = (\alpha + 2)E_0$. The normalization A is obtained for a given luminosity, which is defined by integrating the specific luminosity over 1 keV to 10 MeV in the rest frame:

$$L \equiv \int_{1 \text{ keV}}^{10 \text{ MeV}} L_{E'} dE' = 4\pi d_L^2 \int_{\frac{1 \text{ keV}}{1+z}}^{\frac{10 \text{ MeV}}{1+z}} EN(E) dE, \quad (6)$$

where E' is the photon energy at the rest frame. We use the relations between the energy flux and specific luminosity

$$EN(E) = \frac{(1+z)L_{E'}}{4\pi d_L^2}, \quad (7)$$

and between the photon energies at the observer and rest frames $E = E'/(1+z)$ in the second equality. The peak energy is estimated by assuming its empirical correlation with luminosity, the so-called Yonetoku relation (Yonetoku et al. 2004)

$$\frac{L}{10^{52} \text{ erg s}^{-1}} \simeq 2 \times 10^{-5} [E_p (1+z)]^2, \quad (8)$$

where again the photon energy is measured in a unit of keV. Once the spectral parameters are specified for given z and L , the flux of the GRB observed by a detector is calculated by integrating the flux, $EN(E)$, over the detector's energy range. The minimal luminosity is defined

¹ <https://ep.bao.ac.cn/ep/>

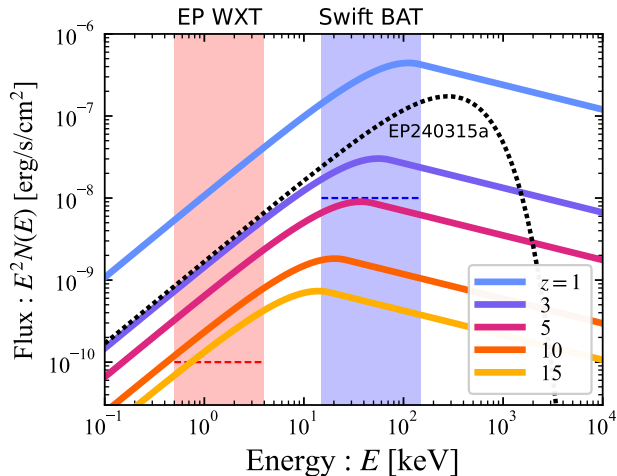


Figure 1. Gamma-ray spectra of a GRB with luminosity $L = 10^{52} \text{ erg s}^{-1}$ at different redshifts. The red and blue shaded regions and dashed lines represent the energy bands and sensitivities of EP WXT and *Swift* BAT, respectively. The black dotted curve shows the spectrum of EP240315a with $L \simeq 1.2 \times 10^{53} \text{ erg s}^{-1}$ and $z \simeq 4.9$ (Liu et al. 2024).

by the luminosity giving the same flux as the detector’s sensitivity. In Table 1, we show the limiting sensitivity and other properties of *Swift* BAT and EP WXT as well as new and future missions. Conservatively we set the fiducial value of EP sensitivity as $\simeq 10^{-10} \text{ erg s}^{-1} \text{ cm}^2$ (obtained by an exposure time of $\simeq 100 \text{ s}$), while its maximal sensitivity is $\simeq 2.6 \times 10^{-11} \text{ erg s}^{-1} \text{ cm}^2$ achieved for $\simeq 1000 \text{ s}$ of exposure.

Figure 1 depicts the flux of a GRB with $L = 10^{52} \text{ erg s}^{-1}$ for different z . The shaded regions and horizontal dashed lines represent the energy band and sensitivity of *Swift* BAT and EP WXT, respectively. Flux in the low energy band is not significantly reduced compared to the high energy band for increasing z (see also Ghirlanda et al. 2015; Palmerio & Daigne 2021). This is because the spectrum has a rising shape at low energy, and the spectral peak decreases not only in flux but also in energy for higher redshift (see Eq. 8). Both effects result in a moderate flux reduction in the low energy band. A similar effect was pointed out by Ciardi & Loeb (2000) for afterglow emissions and observationally confirmed by Frail et al. (2006) for radio afterglows.

We remark that the power-law spectrum of the Band function in soft energy can be extrapolated to EP’s band range. This is supported by the simultaneous detection of EP240315a, a GRB at $z \simeq 4.9$ with $L \simeq 1.2 \times 10^{53} \text{ erg s}^{-1}$ (black dotted curve in Fig. 1), with *Swift* BAT (see Fig. 2b of Liu et al. 2024). The recently reported detection of EP240219a with *Fermi* GBM also supports such an extrapolation (Yin et al. 2024).

The intrinsic GRB formation rate, $\Psi_{\text{GRB}}(z)$, and LF, dn/dL , in Eq. (3) are not well understood. In fact, one of the goals of the GRB population study is to determine them by fitting the distribution of observables such as flux, peak energy, and redshift (Wijers et al. 1998; Krumholz et al. 1998; Mao & Mo 1998; Blain & Natarajan 2000; Porciani & Madau 2001; Lloyd-Ronning et al. 2002; Firmani et al. 2004; Natarajan et al. 2005; Guetta et al. 2005; Jakobsson et al. 2006; Daigne et al. 2006; Salvaterra & Chincarini 2007; Le & Dermer 2007; Chary et al. 2007; Kistler et al. 2008; Li 2008; Yüksel et al. 2008; Kistler et al. 2009; Salvaterra et al. 2009a; Wang & Dai 2009; Qin et al. 2010; Wanderman & Piran 2010; Ishida et al. 2011; Virgili et al. 2011; Robertson & Ellis 2012; Salvaterra et al. 2012; Wang 2013; Sun et al. 2015; Petrosian et al. 2015; Perley et al. 2016; Lan et al. 2019, 2021; Palmerio & Daigne 2021; Ghirlanda & Salvaterra 2022). These population studies commonly parameterize the GRB rate and LF assuming their functional forms and determine them by reproducing the observables. While these functional forms differ for each work, a general conclusion is that if the redshift evolution of the LF is taken into account, the rate and LF are degenerate (e.g., Salvaterra & Chincarini 2007; Qin et al. 2010; Virgili et al. 2011; Salvaterra et al. 2012; Palmerio & Daigne 2021; Ghirlanda & Salvaterra 2022). With the current sample, it is still difficult to break the degeneracy. Therefore, in this work we adopt several parameterized GRB rate and LF found by recent representative population studies (Lan et al. 2021; Palmerio & Daigne 2021; Ghirlanda & Salvaterra 2022) to discuss the detectability of high- z GRBs by EP.

Before describing the details of the works, we remark on the general nature of the GRB rate. GRB rate can be related to the star formation rate (SFR) since long GRBs are produced by the death of short-lived massive stars (e.g., Wijers et al. 1998; Blain & Natarajan 2000; Porciani & Madau 2001; Yüksel et al. 2008; Kistler et al. 2009; Robertson & Ellis 2012). Here we assume that the GRB formation rate is related with the cosmic SFR density at each redshift by

$$\Psi_{\text{GRB}}(z) = \eta_{\text{GRB}}(z) \rho_{\text{SFR}}(z), \quad (9)$$

where η_{GRB} represents the efficiency of GRB formation per stellar mass. Since the GRB formation rate and SFR density have different units, the efficiency has a unit of $[\text{M}_{\odot}^{-1}]$. The observations before the advent of JWST (we call “pre-JWST”) found that the SFR density declines with higher redshift (e.g., Bouwens et al. 2015; Finkelstein et al. 2015; Harikane et al. 2018, 2022). Specifically, as a baseline, we take ρ_{SFR} in Harikane et al. (2022, 2024b) as shown in Fig. 2, whose behavior is understood by structure formation in ΛCDM cosmology with a constant star formation efficiency. We emphasize that most GRB population studies have adopted the SFR density proposed by Madau & Dickinson (2014) (gray

Table 1. The properties of current and future GRB missions.

Detector	Energy range [keV]	Field of view (Ω) [str]	Sensitivity [erg/s/cm ²]	Ref.
Swift BAT	15 – 150	1.4	10^{-8}	Barthelmy et al. (2005)
Einstein Probe WXT	0.5 – 4	1.1	$\sim 10^{-10}$	Yuan et al. (2022)
SVOM ECLAIRs	4 – 150	2	10^{-9}	Wei et al. (2016)
HiZ-GUNDAM	0.5 – 4	0.5	10^{-10}	Yonetoku et al. (2024)
THESEUS SXI	0.3 – 5	0.5	10^{-10}	Amati et al. (2018, 2021)
THESEUS XGIS	2 – 10000	2	10^{-8}	Amati et al. (2018, 2021)
Gamov Explore LEXT	0.5 – 5	0.75	10^{-10}	White (2020)

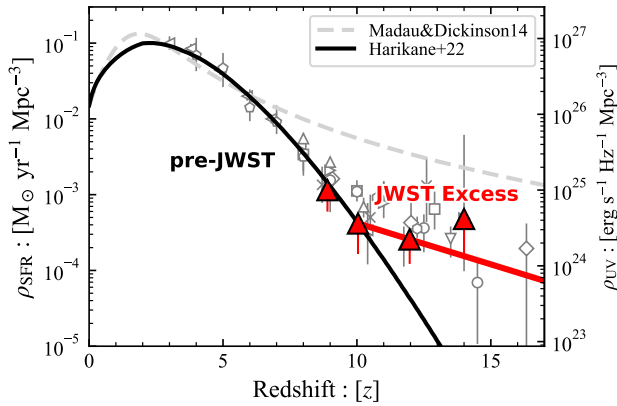


Figure 2. The evolution of the cosmic SFR density. The black curve shows the SFR density obtained in the “pre-JWST” era. The red triangles denote the lower limit of the SFR density estimated by the spectroscopically-confirmed galaxy sample obtained by JWST in Harikane et al. (2024b). The gray open points also show the SFR density obtained by other observations, taken from Harikane et al. (2024b). The SFR density shows an excess beyond $z \gtrsim 10$, which we call the “JWST excess” and may be represented by the red solid line. The gray dashed curve shows the SFR density of Madau & Dickinson (2014), which is frequently used in GRB population studies. The SFR density is estimated by multiplying the conversion factor to the UV luminosity density (on the right axis, see text).

dashed curve) or Hopkins & Beacom (2006). However, it overshoots the observed SFR density beyond $z \gtrsim 6$.

Remarkably, as shown in Fig. 2, the JWST revealed that the SFR density beyond $z \gtrsim 10$ is higher than the extrapolation of the pre-JWST results (Finkelstein et al. 2022, 2023, 2024; Naidu et al. 2022; Adams et al. 2023, 2024; Bouwens et al. 2023a,b; Castellano et al. 2023; Donnan et al. 2023b,a, 2024; Harikane et al. 2023a, 2024a,b; Pérez-González et al. 2023; McLeod et al. 2024; Robertson et al. 2024). Note that these JWST studies measure the UV luminosity density (the right axis

of Fig. 2) and convert it to the SFR density by using galaxy SED models. A commonly used conversion factor is calculated for a stellar population with solar metallicity and the Salpeter initial mass function (IMF, Salpeter 1955) for $0.1 - 100 M_{\odot}$. With a typical conversion factor of $1.15 \times 10^{-28} M_{\odot} \text{ yr}^{-1} / (\text{erg s}^{-1} \text{ Hz}^{-1})$ (e.g., Madau & Dickinson 2014), the overabundance of luminous galaxies is translated to an excess of SFR density over the pre-JWST extrapolation. This JWST excess is shown as a red solid line in Fig. 2, which is obtained by just connecting two data points at $z = 10$ and 12 and extrapolating the line. However, this line could represent a minimal density because the data points are the lower limits. If the JWST excess really reflects an excess of the SFR density, it may also increase the GRB event rate, which is explored in the next section.

In this Letter, we first adopt the GRB formation rate and LF obtained by Ghirlanda & Salvaterra (2022), hereafter GS22, as a representative (we also do the same calculation for the functions in Lan et al. 2021; Palmerio & Daigne 2021 and obtained similar results; see Appendix A). GS22 analyzed the GRB sample obtained by *Swift* BAT up to 2014 (Salvaterra et al. 2012; Pescalli et al. 2016) to reproduce its statistical properties. They adopted a broken power-law LF defined for $L > 10^{47} \text{ erg s}^{-1}$ with a redshift-evolving break luminosity:

$$\frac{dn}{dL} \propto \begin{cases} L^{-p_1} & : L \leq L_b, \\ L^{-p_2} & : L_b < L, \end{cases} \quad (10)$$

$$L_b = L_*(1+z)^k, \quad (11)$$

and obtained $p_1 = 0.97$, $p_2 = 2.21$, $L_* = 10^{52.02} \text{ erg s}^{-1}$, and $k = 0.64$. For the GRB formation rate, they assumed that it has the same functional form as the SFR density of Madau & Dickinson (2014):

$$\Psi_{\text{GRB}} = \Psi_{\text{GRB},0} \frac{(1+z)^{q_1}}{1 + \left(\frac{1+z}{q_2}\right)^{q_3}}, \quad (12)$$

and obtained $\Psi_{\text{GRB},0} = 79 \text{ Gpc}^{-3} \text{ yr}^{-1}$, $q_1 = 3.33$, $q_2 = 3.42$, $q_3 = 6.21$. It should be noted that they

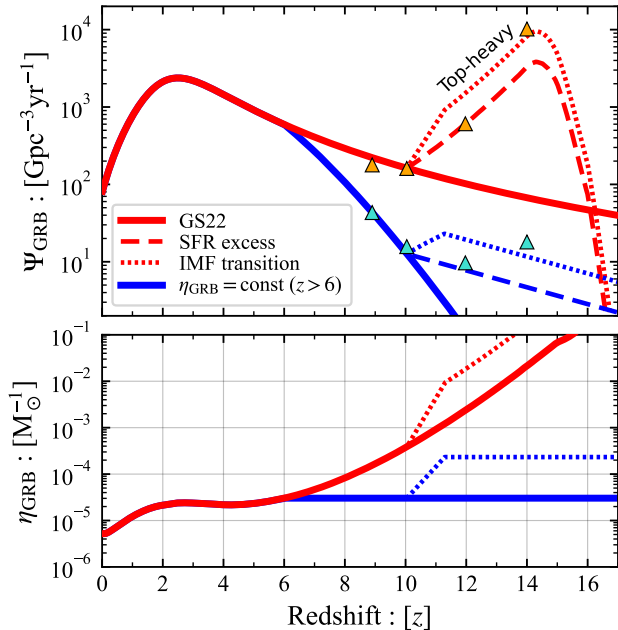


Figure 3. (Top) Intrinsic (beaming-corrected) GRB formation rate for different scenarios. Red and blue solid curves show the rate of Ghirlanda & Salvaterra 2022 (GS22) and the rate extended beyond $z > 6$ in proportion to the pre-JWST SFR. The latter overlaps with the former below $z < 6$, and has a constant GRB formation efficiency η_{GRB} . Dashed curves show the same as the solid ones but boosted in proportion to the SFR excess for $z > 10$. Orange and light-blue triangles represent the GRB-rate excess corresponding to the JWST excess (see Fig. 2) in this scenario. Dotted curves show the case where the JWST excess is caused by a transition of IMF from Salpeter to top-heavy shape over $10 \lesssim z \lesssim 11.3$. For the models of the SFR excess (red dashed) and IMF transition (red dotted), Ψ_{GRB} is artificially suppressed for $z \gtrsim 14$. (Bottom) GRB formation efficiency corresponding to models in the top panel, defined by Eq. (9) for the pre-JWST SFR, ρ_{SFR} (black curve in Fig. 2).

varied the jet opening angle event by event according to an empirical correlation between the angle and radiated gamma-ray energy. On the other hand, we assume a constant jet opening angle for all events, which may not affect the result significantly given the weak dependence² of θ_j on L suggested by the correlation $\theta_j \propto L^{-0.06}$ (but see also Lloyd-Ronning et al. 2020).

² This scaling is obtained by combining the so-called Ghirlanda relation $E_p \propto (\eta_{\text{beam}} E_{\gamma, \text{iso}})^{0.7}$ (Ghirlanda et al. 2007), where $E_{\gamma, \text{iso}}$ is the isotropic equivalent gamma-ray energy, Amati relation $E_p \propto E_{\gamma, \text{iso}}^{0.6}$ (Amati et al. 2002), and Yonetoku relation of Eq. (8).

Figure 3 shows the GRB formation rate obtained by GS22 and the corresponding formation efficiency (η_{GRB} , Eq. 9) calculated for “pre-JWST” SFR density (Fig. 2). The efficiency weakly increases for $z \lesssim 3$, which is interpreted by the facts that GRBs preferentially occur in low-metal galaxies, and that cosmic metallicity decreases for higher redshift (e.g., Langer & Norman 2006). We stress that the GRB sample analyzed by GS22 contains bursts only up to $z \lesssim 6$, and Ψ_{GRB} beyond $z \gtrsim 6$ is not calibrated with observations but just an extrapolation of Eq. (12). Actually the efficiency increases again for $z \gtrsim 6$ to as high as $\eta_{\text{GRB}} \sim 10^{-2}$, which corresponds to an extreme situation where most massive stars collapse to BH and produce GRB. This may be artificial and only reflect the discrepancy between the SFR formula of Madau & Dickinson (2014) and the observed pre-JWST SFR density. However, we still adopt this formation rate to estimate the high- z GRB event rate as the *most optimistic* model.³

A more conservative GRB rate may be obtained by extending Ψ_{GRB} of GS22 from $z \simeq 6$ in proportion to the pre-JWST SFR density with a constant η_{GRB} as in Eq. (9). This scenario is depicted in a thick blue solid curve in Fig. 3. We remark that the GRB detection rate calculated by this formation rate gives a negligibly small detection rate at $z \simeq 8 - 9$ for *Swift* BAT, while it detected several such GRBs; GRB 090423 at $z = 8.2$ (Salvaterra et al. 2009b; Tanvir et al. 2009) and GRB 090429 at $z \simeq 9.4$ (Cucchiara et al. 2011). Therefore, we may regard this scenario as the *most conservative* model.

3. GRB FORMATION RATES AND THE JWST EXCESS

Including the above two cases, there are several possibilities on the evolution of Ψ_{GRB} for $z \gtrsim 10$. They are motivated by different scenarios of the origin of the JWST excess in the SFR density (Fig. 2). These scenarios can be summarized as follows:

- **Case A: SFR excess.** A real elevation of the SFR can cause the JWST excess. Such an efficient star formation at $z \gtrsim 10$ is expected via e.g., the feedback-free (Dekel et al. 2023; Li et al. 2023) and compact star formation (e.g., Fukushima & Yajima 2021). Note that here the conversion factor from the UV luminosity to SFR does not evolve in time (in contrast to case B discussed below), and the star formation efficiency should be larger than the pre-JWST one found in Harikane et al.

³ We note that the recent measurement of a low oxygen-to-iron ratio at a galaxy at $z \simeq 10.6$ may suggest that collapsars or hypernovae are frequent (Nakane et al. 2024).

(2022).⁴ In this case A, the GRB formation rate is also elevated in the same amount as the SFR according to Eq. (9) because an IMF does not change. The corresponding GRB formation rates are shown by dashed curves in the upper panel of Fig. 3 as deviations from GS22 (red solid) and $\eta_{\text{GRB}} = \text{const}$ models (blue solid curve).

- **Case B: IMF transition.** A transition of the Salpeter IMF to top-heavy one increases the conversion factor from the UV luminosity to SFR, which may result in the JWST excess without a genuine excess of the SFR (Chon et al. 2022; Inayoshi et al. 2022; Steinhardt et al. 2023). For example, Harikane et al. (2023a) demonstrated that the conversion factor becomes $\simeq 3$ times higher for a top-heavy IMF than Salpeter one (see their Figure 20, and Table 1 of Inayoshi et al. 2022 for details).

We construct Ψ_{GRB} in this scenario by assuming that the IMF gradually shifts to a top-heavy shape while the true SFR density traces the pre-JWST one. However, with the same parameters as Inayoshi et al. (2022), we find that for the IMF transition alone cannot sustain the JWST excess beyond $z \gtrsim 11.3$, and hence an excess of the true SFR is still required (but $\simeq 3$ times lower than the JWST excess in Fig. 2 due to more efficient UV emissivity). Importantly, more abundant massive stars boost the GRB formation efficiency. We may factor out the effect of the IMF on the efficiency as

$$\eta_{\text{GRB}} \propto \frac{\int_{m_{\text{GRB}}}^{m_{\text{up}}} \phi(m) dm}{\int_{m_{\text{low}}}^{m_{\text{up}}} m \phi(m) dm}, \quad (13)$$

where $\phi(m)$ is the IMF defined for $m_{\text{low}} < m < m_{\text{up}}$, and m_{GRB} is the minimal mass to produce a GRB (we set $m_{\text{GRB}} = 25 M_{\odot}$ following de Souza et al. 2011). For the Salpeter and top-heavy⁵ IMFs in Inayoshi et al. (2022), this factor takes values of $\simeq 1.4 \times 10^{-3}$ and $\simeq 1.1 \times 10^{-2}$, respectively. Therefore, when the IMF completes the transition at $z \simeq 11.3$, the GRB formation efficiency becomes $1.1/0.14 \simeq 7.9$ times higher than that at $z \simeq 10$. This increase of η_{GRB} results in an overall increase of the GRB formation rate by $7.9/3 \simeq 2.6$ times

⁴ Such intense star formation may cause radiation-drive winds, which clear up dust from galaxies and play a role to shape the bright end in the UV luminosity function (Ferrara et al. 2023; Tsuna et al. 2023; Ferrara 2024).

⁵ Inayoshi et al. (2022) considered a log normal distribution defined from $1 M_{\odot}$ to $500 M_{\odot}$ with a mean mass of $10 M_{\odot}$ dispersion of M_{\odot} . In the estimation of η_{GRB} , we excluded a mass window of pair instability supernovae, $140 - 260 M_{\odot}$ (e.g., Heger & Woosley 2002).

higher than the case A beyond $z \gtrsim 11.3$ (here the denominator, 3 comes from the reduction of the SFR from the value in case A). Ψ_{GRB} of this scenario are shown by dotted curves in Fig. 3. Note we simply interpolate Ψ_{GRB} in the transition period ($10 \lesssim z \lesssim 11.3$), although an actual shape depends on how the IMF changes over the period.

- **Case C: AGN.** Our last possibility is related not directly with star formation processes but other effects such as contribution from active galactic nuclei (AGNs, Harikane et al. 2023b; Hegde et al. 2024). The corresponding GRB formation rates are actually already represented by the original GS22 (red solid) and $\eta_{\text{GRB}} = \text{const}$ models as the red and blue solid curves in Fig. 3. This is because the SFR nor GRB formation efficiency should not be increased to cause the JWST excess.

Note that while above three possibilities are listed up independently, they may be related with each other and interplay to shape the GRB formation rate. For instance, abundant massive stars born through a top-heavy IMF would cause an intense feedback diminishing the star formation efficiency (Chon et al. 2024; Menon et al. 2024). Nevertheless in this Letter we consider them separately as idealized cases and to see individual effects.

4. RESULTS

Figure. 4 shows the redshift distribution and cumulative number of detected GRBs expected for the observation by EP. Within the models of GS22, the total number of GRB detection expected for one-year operation amounts to $\simeq 280$ (see the bottom panel in Fig. 4), which could be larger than the actual number. As of September 1, 2024, $\simeq 30$ X-ray transients have been reported on GCN circulars⁶, corresponding to $\simeq 50$ events per year, although currently not all detections are being reported and the instrument characteristics are still being investigated. In addition, our choice of the limiting flux, $\sim 10^{-10} \text{ erg s}^{-1} \text{ cm}^{-2}$, may not be applicable to compare our estimate with the current detection number since the observation by EP has just started and it underwent a commission phase. Another possibility is that a jet opening angle might be smaller than our fiducial value of $\theta_j = 0.1$. The detection of EP240315a at $z \simeq 4.9$ only two months after the start of operation (Liu et al. 2024), may also put a lower limit on the detection rate at $z \sim 5$ (corresponding to 6 events per year, upward triangle).⁷

If the original GRB formation rate of GS22 can be extrapolated beyond $z \gtrsim 6$ (red solid curve), a few GRBs

⁶ <https://gcn.nasa.gov/circulars>

⁷ If the first month after the launch of EP was not available for observation, the rate could be doubled.

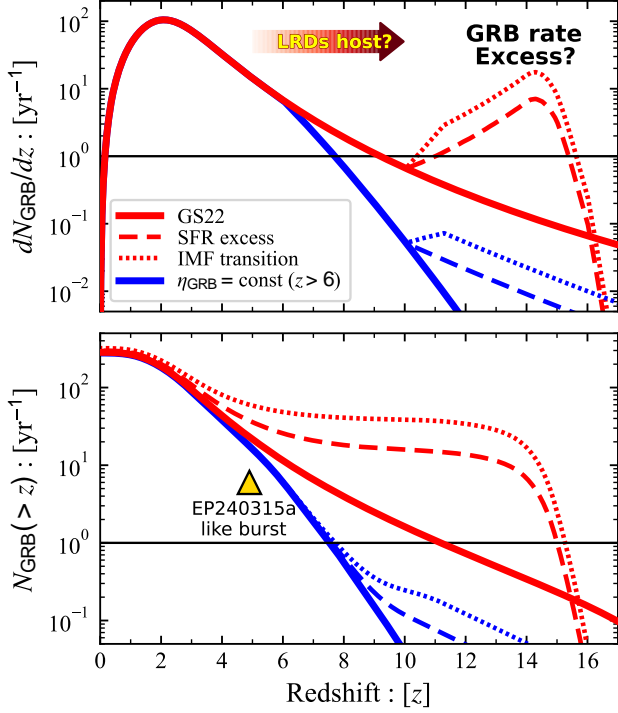


Figure 4. (Top) Prediction for the redshift distribution of GRBs detected by EP. Color and types of curves correspond to the same meaning as in Fig. 3. The upper arrow represents a redshift range over which little red dots (LRDs) might be a host galaxy of GRBs, see discussion in Sec. 5. (Bottom) The cumulative number of GRBs detected by EP. The upward triangle means an expected lower-limit based on the detection of EP240315a.

at $z \geq 10$ could be detected for one-year observation. The number of detection could be ten times larger if the JWST excess caused by the SFR excess or IMF transition; in these cases, one GRB could be detected per a few years even for the conservative model adopting $\eta_{\text{GRB}} = \text{const}$ (blue solid curve). More specific detection numbers are shown in Table 2.

More interestingly, the redshift distribution of GRBs can show an excess from an extrapolation from low redshifts or even increases for $z \gtrsim 10$ depending on the origins of the JWST excess, which will be useful in discriminating the models. In case A (dashed curves in Fig. 4), the excess of the SFR also causes an excess of the GRB event rate in proportion to the SFR. In case B (dotted curves), the GRB rate increases more rapidly than case A during the period of the IMF transition ($10 \lesssim z \lesssim 11.3$). In case C (solid curves), the true SFR and GRB efficiency do not have an excess from the pre-JWST value, and hence the GRB rate extends smoothly as an extrapolation of the rate at $z \lesssim 10$.

Figure 5 summarizes the above discussion about a potential behavior of the high- z GRB rate, and its impli-

Table 2. Cumulative detection numbers of GRBs by EP in our each model.

Model	Cumulative number $N_{\text{GRB}}(> z)$ [yr^{-1}]		
	$z = 8$	$z = 10$	$z = 12$
GS22	4	2	0.7
+SFR excess	18	16	14
+IMF transition	41	39	34
$\eta_{\text{GRB}} = \text{const} (z > 6)$	0.6	0.04	0.002
+SFR excess	0.6	0.1	0.05
+IMF transition	0.8	0.2	0.1

Origin of the JWST excess probed by high- z GRBs

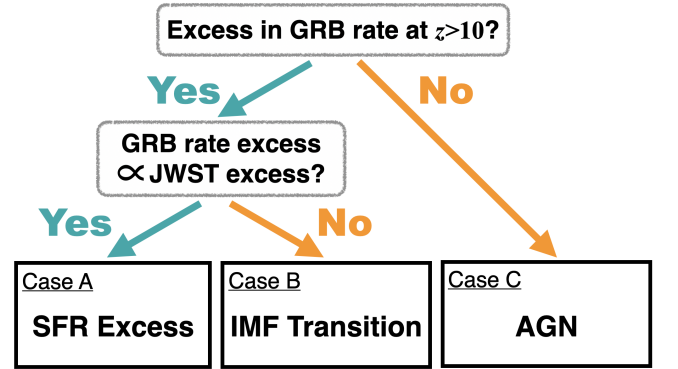


Figure 5. Origin of the JWST excess implied by the behavior of the GRB event rate for $z \gtrsim 10$. If the GRB rate shows an excess at $z \gtrsim 10$ proportional to the JWST excess (the red or blue dashed curves in Fig. 4), an excess of the SFR is an origin of the JWST excess (Case A). If the GRB rate shows an excess larger than the JWST excess (the red or blue dotted curves), the IMF transition causes the JWST excess (Case B). If there is no excess in the GRB rate (the red or blue solid curves), AGN activity is responsible to the JWST excess (Case C).

cation on the origin of the JWST excess. If an excess in the GRB redshift distribution is identified at $z \gtrsim 10$, it suggests that the JWST excess is caused by a real elevation of the SFR from the pre-JWST value (case A) or a transition of IMF from Salpeter to top-heavy ones (case B). These scenarios could be discriminated by the amount of the increase in the GRB rate. No detection of an excess in the GRB rate supports that the JWST excess is caused by contribution from AGNs (case C).

5. DISCUSSION & SUMMARY

In this Letter, we explore the detectability of high- z GRBs by WXT onboard EP, which started its operation in January 2024. Owing to the high sensitivity at

the soft X-ray band, WXT is an ideal detector to access high- z GRBs as demonstrated for EP240315a (Liu et al. 2024). We find that EP could detect a few GRBs at $z \geq 10$ for a one-year operation if the GRB formation rate calibrated by GRBs at $z \lesssim 6$ can be extrapolated to $z \simeq 10$. In particular, we focus on a synergy with JWST, which has recently reported an excess in the UV luminosity density and SFR density at $z \gtrsim 10$ (e.g., Harikane et al. 2024b). Since long GRBs are produced by collapse of massive stars, they probe the star formation activities in high- z universe by directly tracing the star formation history. Interestingly, depending on potential origins of the JWST excess, the redshift distribution of GRBs shows different behaviors (Fig. 4). As summarized in Fig. 5, if the JWST excess is caused by an elevation of the genuine SFR (case A), the redshift distribution has an excess at $z \gtrsim 10$ in proportion to the JWST excess. If the transition of IMF from Salpeter to top-heavy one creates the JWST excess (case B), the distribution also shows an excess but the degree of the excess is different from case A. If other effects than star formation activities such as AGN contribution (case C), the distribution extends smoothly beyond $z \gtrsim 10$.

It should be noted that EP alone, as an X-ray telescope, cannot determine redshift, and followups in optical and NIR wavelengths are critical to identify high- z GRBs. Such followups may not be always possible for observation by EP, which may lower the number of detection than our estimates. Recently launched SVOM and future missions (see Table 1) with their own follow-up telescopes will play a role in the detection of high- z GRBs (e.g., see Llamas Lanza et al. 2024, for the prospect of SVOM).

The nature of high- z GRB’s host galaxies is poorly understood, and their detection will be profitable (Tanvir et al. 2012; McGuire et al. 2016; Sears et al. 2024). Remarkably for most GRBs beyond $z > 6$, only absorption by ISM in optical afterglow has been observed, and the emission from galaxies is hardly detected (McGuire et al. 2016). We speculate that JWST-discovered puzzling galaxies, the so-called little red dots (LRDs, Harikane et al. 2023b; Kocevski et al. 2023; Labbé et al. 2023; Matthee et al. 2024) might be host galaxies of GRBs. LRDs are characterized by an extremely red rest-optical SED and compact size, and their origin is a mystery. Currently discussed possibilities include dust-obscured star-forming galaxies and AGNs. We propose that LRDs may represent a non-negligible fraction of high- z GRB

hosts, if they are star-forming galaxies. Some SED modeling of LRDs finds that the SFR is as high as $\sim 10^{2-3} M_{\odot} \text{ yr}^{-1}$ (Xiao et al. 2023; Pérez-González et al. 2024), which is 10-100 times higher than typical galaxies ($1 - 10 M_{\odot} \text{ yr}^{-1}$). Although the number density is $\sim 10^{-2}$ times lower than normal Lyman break galaxies (Greene et al. 2024; Kocevski et al. 2024; Kokorev et al. 2024; Matthee et al. 2024), the potential high SFR suggests that they could at least partly contribute not only to the SFR density at a comparable level to normal galaxies (Xiao et al. 2023) but also to the GRB formation rate. GRBs hosted by LRDs would not show an afterglow in optical wavelengths shorter than $\lesssim 0.73 \left(\frac{1+z}{6}\right) \mu\text{m}$ due to Lyman- α absorption, but they could be bright in NIR; hence JWST followup observations of “dark” GRBs (e.g., Fynbo et al. 2001) with NIR counterparts may test this possibility.

Finally, detecting binary black hole (BBH) mergers at high redshifts might also be helpful to elucidate the origin of the JWST excess. BBH progenitors may experience GRBs (e.g., Marchant et al. 2016) while recent studies found that the fraction of GRBs evolving into a BBH detected by LIGO/Virgo is minor (e.g., Arcier & Atteia 2022; Wu & Fishbach 2024). However, since BBHs originate from massive stars, regardless of the connection with GRBs, their merger rate or mass distribution at high- z may contain a hint to the JWST excess. In particular, unless the delay-time distribution is significantly shallow, the BBH merger rate would have an excess as in case A, and mass distribution would have a top-heavy shape in case B. Cosmic Explorer (Reitze et al. 2019) and Einstein Telescope (Punturo et al. 2010) will provide ideal opportunities to test these scenarios.

1 We thank Bing Zhang for stimulating discussion. We
 2 also thank the Yukawa Institute for Theoretical Physics
 3 at Kyoto University and participants to the YITP
 4 workshop YITP-W-24-22 on “Exploring Extreme Tran-
 5 sients: Emerging Frontiers and Challenges”. Discus-
 6 sions in the workshop were helpful to complete this
 7 work. This research is supported by the Hakubi
 8 project at Kyoto University, JSPS KAKENHI grant
 9 No. JP24K17088 (T.M.), JP24H00245, JP22K21349
 10 (Y.H.), JP24H01810, JP24K00682, JP20H00174
 11 (K.M.), MEXT/JSPS KAKENHI grant No. 23H01172,
 12 23H05430, 23H04900, 22H00130, 20H01901, 20H01904,
 13 and 20H00158 (K.I.).

APPENDIX

A. OTHER GRB FORMATION RATE AND LF

We briefly discuss the results for other GRB formation rate and LF. As other representative studies of the GRB population than GS22, we consider Lan et al. (2021) and Palmerio & Daigne (2021). These works did not derive the intrinsic GRB formation rate Ψ_{GRB} , but the rate for on-axis GRBs, which is expressed by $\eta_{\text{beam}} \Psi_{\text{GRB}}$ in our notation.

Lan et al. 2021 analyzed 302 GRBs detected by Swift up to 2019 with a photon count rate greater than $\geq 1 \text{ photons s}^{-1} \text{ cm}^{-2}$. They assumed that the (on-axis) GRB formation rate is proportional to the SFR as in Eq. (9), and a broken power-law LF (Eq. 10, defined for $10^{49} \text{ erg s}^{-1} < L < 10^{55} \text{ erg s}^{-1}$). Several possibilities were considered such as combinations of both non-evolving GRB formation efficiency ($\eta_{\text{GRB}} = \text{const}$) and LF ($k = 0$), and either redshift-evolving efficiency or LF. We consider their result for the GRB formation rate with an evolving efficiency:

$$\eta_{\text{beam}} \Psi_{\text{GRB}} = 37.9(1+z)^{1.43} \left[\frac{0.0157 + 0.118z}{1 + \left(\frac{z}{3.23}\right)^{4.66}} \right] \text{Gpc}^{-3} \text{yr}^{-1}, \quad (\text{A1})$$

where the bracketed factor comes from the SFR of Hopkins & Beacom (2006); Li (2008), and the other factor shows the z -dependence of the GRB formation efficiency. The LF is assumed to be independent of redshift ($k = 0$) and its parameters are obtained as $p_1 = 0.60$, $p_2 = 1.65$, and $L_* = 10^{52.98} \text{ erg s}^{-1}$.

Palmerio & Daigne 2021 modeled the same GRB sample as Ghirlanda & Salvaterra (2022). They parameterized the GRB formation rate as:

$$\eta_{\text{beam}} \Psi_{\text{GRB}}(z) = \tilde{\Psi}_{\text{GRB},0} \begin{cases} e^{az} & : z \leq z_m, \\ e^{bz} e^{(a-b)z_m} & : z > z_m, \end{cases} \quad (\text{A2})$$

whose functional form is motivated by the cosmic SFR. They considered a Schechter LF (Schechter 1976, defined for $L > 5 \times 10^{49} \text{ erg s}^{-1}$) with redshift evolving break:

$$\frac{dn}{dL} \propto \left(\frac{L}{L_b}\right)^{-p} \exp\left(-\frac{L}{L_b}\right), \quad (\text{A3})$$

where the break luminosity is defined by Eq. (11). They did not determine the strength of z -evolution of the break luminosity k by fit, but considered cases of $k = 0, 0.5, 1$, and 2 . All cases give a reasonable fit, and we adopt the case of $k = 1$ as a moderate value. In this case, the parameters are obtained as $\tilde{\Psi}_{\text{GRB},0} = 0.72 \text{ Gpc}^{-3} \text{yr}^{-1}$, $a = 1.2$, $b = -0.27$, $z_m = 2.1$, $p = 1.47$, and $L_* = 10^{52.9} \text{ erg s}^{-1}$.

Figure 6 shows the redshift distribution and cumulative number of GRBs detected by EP for the cases of Lan et al. (2021) and Palmerio & Daigne (2021). While the adopted GRB formation rate and LF are different from GS22, the results are qualitatively similar. The absolute values of detection rate for Lan et al. (2021) is ~ 10 times larger than GS22 and Palmerio & Daigne (2021), and it will be easily constrained by observations. The agreement between GS22 and Palmerio & Daigne (2021) might support our choice of the opening angle of $\theta_j = 0.1$ if Lan et al. (2021) is excluded in the future observations.

REFERENCES

- Adams, N. J., Conselice, C. J., Ferreira, L., et al. 2023, MNRAS, 518, 4755, doi: [10.1093/mnras/stac3347](https://doi.org/10.1093/mnras/stac3347)
- Adams, N. J., Conselice, C. J., Austin, D., et al. 2024, ApJ, 965, 169, doi: [10.3847/1538-4357/ad2a7b](https://doi.org/10.3847/1538-4357/ad2a7b)
- Amati, L., Frontera, F., Tavani, M., et al. 2002, A&A, 390, 81, doi: [10.1051/0004-6361:20020722](https://doi.org/10.1051/0004-6361:20020722)
- Amati, L., O'Brien, P., Götz, D., et al. 2018, Advances in Space Research, 62, 191, doi: [10.1016/j.asr.2018.03.010](https://doi.org/10.1016/j.asr.2018.03.010)
- Amati, L., O'Brien, P. T., Götz, D., et al. 2021, Experimental Astronomy, 52, 183, doi: [10.1007/s10686-021-09807-8](https://doi.org/10.1007/s10686-021-09807-8)
- Arcier, B., & Atteia, J.-L. 2022, ApJ, 933, 17, doi: [10.3847/1538-4357/ac6604](https://doi.org/10.3847/1538-4357/ac6604)
- Band, D., Matteson, J., Ford, L., et al. 1993, ApJ, 413, 281, doi: [10.1086/172995](https://doi.org/10.1086/172995)
- Barthelmy, S. D., Barbier, L. M., Cummings, J. R., et al. 2005, SSRv, 120, 143, doi: [10.1007/s11214-005-5096-3](https://doi.org/10.1007/s11214-005-5096-3)
- Blain, A. W., & Natarajan, P. 2000, MNRAS, 312, L35, doi: [10.1046/j.1365-8711.2000.03318.x](https://doi.org/10.1046/j.1365-8711.2000.03318.x)
- Bouwens, R., Illingworth, G., Oesch, P., et al. 2023a, MNRAS, 523, 1009, doi: [10.1093/mnras/stad1014](https://doi.org/10.1093/mnras/stad1014)
- Bouwens, R. J., Illingworth, G. D., Oesch, P. A., et al. 2015, ApJ, 803, 34, doi: [10.1088/0004-637X/803/1/34](https://doi.org/10.1088/0004-637X/803/1/34)
- Bouwens, R. J., Stefanon, M., Brammer, G., et al. 2023b, MNRAS, 523, 1036, doi: [10.1093/mnras/stad1145](https://doi.org/10.1093/mnras/stad1145)
- Bromm, V., & Loeb, A. 2006, ApJ, 642, 382, doi: [10.1086/500799](https://doi.org/10.1086/500799)
- Castellano, M., Fontana, A., Treu, T., et al. 2023, ApJL, 948, L14, doi: [10.3847/2041-8213/accea5](https://doi.org/10.3847/2041-8213/accea5)
- Chary, R., Berger, E., & Cowie, L. 2007, ApJ, 671, 272, doi: [10.1086/522692](https://doi.org/10.1086/522692)

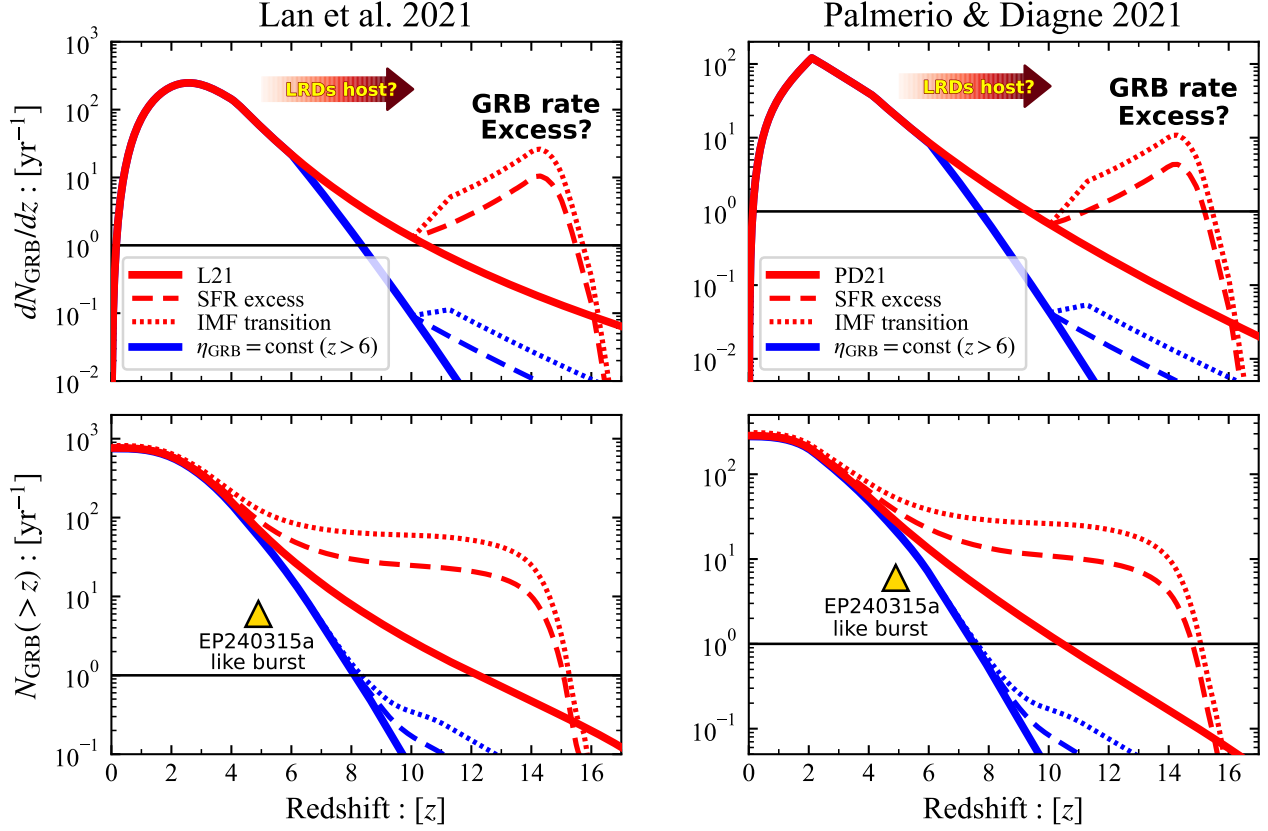


Figure 6. The same as Figs. 3 and 4 but for the GRB formation rate and LF of Lan et al. 2021 (L21, left) and Palmerio & Daigne 2021 (PD21, right), respectively.

Chon, S., Hosokawa, T., Omukai, K., & Schneider, R. 2024, MNRAS, 530, 2453, doi: [10.1093/mnras/stae1027](https://doi.org/10.1093/mnras/stae1027)

Chon, S., Ono, H., Omukai, K., & Schneider, R. 2022, MNRAS, 514, 4639, doi: [10.1093/mnras/stac1549](https://doi.org/10.1093/mnras/stac1549)

Chornock, R., Berger, E., Fox, D. B., et al. 2013, ApJ, 774, 26, doi: [10.1088/0004-637X/774/1/26](https://doi.org/10.1088/0004-637X/774/1/26)

Ciardi, B., & Loeb, A. 2000, ApJ, 540, 687, doi: [10.1086/309384](https://doi.org/10.1086/309384)

Cucchiara, A., Levan, A. J., Fox, D. B., et al. 2011, ApJ, 736, 7, doi: [10.1088/0004-637X/736/1/7](https://doi.org/10.1088/0004-637X/736/1/7)

Daigne, F., Rossi, E. M., & Mochkovitch, R. 2006, MNRAS, 372, 1034, doi: [10.1111/j.1365-2966.2006.10837.x](https://doi.org/10.1111/j.1365-2966.2006.10837.x)

de Souza, R. S., Yoshida, N., & Ioka, K. 2011, A&A, 533, A32, doi: [10.1051/0004-6361/201117242](https://doi.org/10.1051/0004-6361/201117242)

Dekel, A., Sarkar, K. C., Birnboim, Y., Mandelker, N., & Li, Z. 2023, MNRAS, 523, 3201, doi: [10.1093/mnras/stad1557](https://doi.org/10.1093/mnras/stad1557)

Donnan, C. T., McLeod, D. J., McLure, R. J., et al. 2023a, MNRAS, 520, 4554, doi: [10.1093/mnras/stad471](https://doi.org/10.1093/mnras/stad471)

Donnan, C. T., McLeod, D. J., Dunlop, J. S., et al. 2023b, MNRAS, 518, 6011, doi: [10.1093/mnras/stac3472](https://doi.org/10.1093/mnras/stac3472)

Donnan, C. T., McLure, R. J., Dunlop, J. S., et al. 2024, arXiv e-prints, arXiv:2403.03171, doi: [10.48550/arXiv.2403.03171](https://doi.org/10.48550/arXiv.2403.03171)

Fausey, H. M., Vejlggaard, S., van der Horst, A. J., et al. 2024, arXiv e-prints, arXiv:2403.13126, doi: [10.48550/arXiv.2403.13126](https://doi.org/10.48550/arXiv.2403.13126)

Ferrara, A. 2024, A&A, 684, A207, doi: [10.1051/0004-6361/202348321](https://doi.org/10.1051/0004-6361/202348321)

Ferrara, A., Pallottini, A., & Dayal, P. 2023, MNRAS, 522, 3986, doi: [10.1093/mnras/stad1095](https://doi.org/10.1093/mnras/stad1095)

Finkelstein, S. L., Ryan, Russell E., J., Papovich, C., et al. 2015, ApJ, 810, 71, doi: [10.1088/0004-637X/810/1/71](https://doi.org/10.1088/0004-637X/810/1/71)

Finkelstein, S. L., Bagley, M. B., Arrabal Haro, P., et al. 2022, ApJL, 940, L55, doi: [10.3847/2041-8213/ac966e](https://doi.org/10.3847/2041-8213/ac966e)

Finkelstein, S. L., Bagley, M. B., Ferguson, H. C., et al. 2023, ApJL, 946, L13, doi: [10.3847/2041-8213/acade4](https://doi.org/10.3847/2041-8213/acade4)

Finkelstein, S. L., Leung, G. C. K., Bagley, M. B., et al. 2024, ApJL, 969, L2, doi: [10.3847/2041-8213/ad4495](https://doi.org/10.3847/2041-8213/ad4495)

Firmani, C., Avila-Reese, V., Ghisellini, G., & Tutukov, A. V. 2004, ApJ, 611, 1033, doi: [10.1086/422186](https://doi.org/10.1086/422186)

Frail, D. A., Kulkarni, S. R., Sari, R., et al. 2001, ApJL, 562, L55, doi: [10.1086/338119](https://doi.org/10.1086/338119)

- Frail, D. A., Cameron, P. B., Kasliwal, M., et al. 2006, *ApJL*, 646, L99, doi: [10.1086/506934](https://doi.org/10.1086/506934)
- Fukushima, H., & Yajima, H. 2021, *MNRAS*, 506, 5512, doi: [10.1093/mnras/stab2099](https://doi.org/10.1093/mnras/stab2099)
- Fynbo, J. U., Jensen, B. L., Gorosabel, J., et al. 2001, *A&A*, 369, 373, doi: [10.1051/0004-6361:20010112](https://doi.org/10.1051/0004-6361:20010112)
- Gallerani, S., Salvaterra, R., Ferrara, A., & Choudhury, T. R. 2008, *MNRAS*, 388, L84, doi: [10.1111/j.1745-3933.2008.00504.x](https://doi.org/10.1111/j.1745-3933.2008.00504.x)
- Ghirlanda, G., Nava, L., Ghisellini, G., & Firmani, C. 2007, *A&A*, 466, 127, doi: [10.1051/0004-6361:20077119](https://doi.org/10.1051/0004-6361:20077119)
- Ghirlanda, G., & Salvaterra, R. 2022, *ApJ*, 932, 10, doi: [10.3847/1538-4357/ac6e43](https://doi.org/10.3847/1538-4357/ac6e43)
- Ghirlanda, G., Salvaterra, R., Ghisellini, G., et al. 2015, *MNRAS*, 448, 2514, doi: [10.1093/mnras/stv183](https://doi.org/10.1093/mnras/stv183)
- Gillanders, J. H., Rhodes, L., Srivastav, S., et al. 2024, *ApJL*, 969, L14, doi: [10.3847/2041-8213/ad55cd](https://doi.org/10.3847/2041-8213/ad55cd)
- Goldstein, A., Connaughton, V., Briggs, M. S., & Burns, E. 2016, *ApJ*, 818, 18, doi: [10.3847/0004-637X/818/1/18](https://doi.org/10.3847/0004-637X/818/1/18)
- Gou, L. J., Mészáros, P., Abel, T., & Zhang, B. 2004, *ApJ*, 604, 508, doi: [10.1086/382061](https://doi.org/10.1086/382061)
- Greene, J. E., Labbe, I., Goulding, A. D., et al. 2024, *ApJ*, 964, 39, doi: [10.3847/1538-4357/ad1e5f](https://doi.org/10.3847/1538-4357/ad1e5f)
- Greiner, J., Krühler, T., Fynbo, J. P. U., et al. 2009, *ApJ*, 693, 1610, doi: [10.1088/0004-637X/693/2/1610](https://doi.org/10.1088/0004-637X/693/2/1610)
- Guetta, D., & Piran, T. 2007, *JCAP*, 2007, 003, doi: [10.1088/1475-7516/2007/07/003](https://doi.org/10.1088/1475-7516/2007/07/003)
- Guetta, D., Piran, T., & Waxman, E. 2005, *ApJ*, 619, 412, doi: [10.1086/423125](https://doi.org/10.1086/423125)
- Harikane, Y., Nakajima, K., Ouchi, M., et al. 2024a, *ApJ*, 960, 56, doi: [10.3847/1538-4357/ad0b7e](https://doi.org/10.3847/1538-4357/ad0b7e)
- Harikane, Y., Ouchi, M., Ono, Y., et al. 2018, *PASJ*, 70, S11, doi: [10.1093/pasj/psx097](https://doi.org/10.1093/pasj/psx097)
- Harikane, Y., Ono, Y., Ouchi, M., et al. 2022, *ApJS*, 259, 20, doi: [10.3847/1538-4365/ac3dfc](https://doi.org/10.3847/1538-4365/ac3dfc)
- Harikane, Y., Ouchi, M., Oguri, M., et al. 2023a, *ApJS*, 265, 5, doi: [10.3847/1538-4365/acaaa9](https://doi.org/10.3847/1538-4365/acaaa9)
- Harikane, Y., Zhang, Y., Nakajima, K., et al. 2023b, *ApJ*, 959, 39, doi: [10.3847/1538-4357/ad029e](https://doi.org/10.3847/1538-4357/ad029e)
- Harikane, Y., Inoue, A. K., Ellis, R. S., et al. 2024b, *arXiv e-prints*, arXiv:2406.18352, doi: [10.48550/arXiv.2406.18352](https://doi.org/10.48550/arXiv.2406.18352)
- Hartoog, O. E., Malesani, D., Fynbo, J. P. U., et al. 2015, *A&A*, 580, A139, doi: [10.1051/0004-6361/201425001](https://doi.org/10.1051/0004-6361/201425001)
- Hegde, S., Wyatt, M. M., & Furlanetto, S. R. 2024, *arXiv e-prints*, arXiv:2405.01629, doi: [10.48550/arXiv.2405.01629](https://doi.org/10.48550/arXiv.2405.01629)
- Heger, A., & Woosley, S. E. 2002, *ApJ*, 567, 532, doi: [10.1086/338487](https://doi.org/10.1086/338487)
- Hopkins, A. M., & Beacom, J. F. 2006, *ApJ*, 651, 142, doi: [10.1086/506610](https://doi.org/10.1086/506610)
- Inayoshi, K., Harikane, Y., Inoue, A. K., Li, W., & Ho, L. C. 2022, *ApJL*, 938, L10, doi: [10.3847/2041-8213/ac9310](https://doi.org/10.3847/2041-8213/ac9310)
- Ishida, E. E. O., de Souza, R. S., & Ferrara, A. 2011, *MNRAS*, 418, 500, doi: [10.1111/j.1365-2966.2011.19501.x](https://doi.org/10.1111/j.1365-2966.2011.19501.x)
- Jakobsson, P., Levan, A., Fynbo, J. P. U., et al. 2006, *A&A*, 447, 897, doi: [10.1051/0004-6361:20054287](https://doi.org/10.1051/0004-6361:20054287)
- Kaneko, Y., Preece, R. D., Briggs, M. S., et al. 2006, *The Astrophysical Journal Supplement Series*, 166, 298, doi: [10.1086/505911](https://doi.org/10.1086/505911)
- Kashiyama, K., Nakauchi, D., Suwa, Y., Yajima, H., & Nakamura, T. 2013, *ApJ*, 770, 8, doi: [10.1088/0004-637X/770/1/8](https://doi.org/10.1088/0004-637X/770/1/8)
- Kawai, N., Kosugi, G., Aoki, K., et al. 2006, *Nature*, 440, 184, doi: [10.1038/nature04498](https://doi.org/10.1038/nature04498)
- Kinugawa, T., Harikane, Y., & Asano, K. 2019, *ApJ*, 878, 128, doi: [10.3847/1538-4357/ab2188](https://doi.org/10.3847/1538-4357/ab2188)
- Kistler, M. D., Yüksel, H., Beacom, J. F., Hopkins, A. M., & Wyithe, J. S. B. 2009, *ApJL*, 705, L104, doi: [10.1088/0004-637X/705/2/L104](https://doi.org/10.1088/0004-637X/705/2/L104)
- Kistler, M. D., Yüksel, H., Beacom, J. F., & Stanek, K. Z. 2008, *ApJL*, 673, L119, doi: [10.1086/527671](https://doi.org/10.1086/527671)
- Kocevski, D. D., Onoue, M., Inayoshi, K., et al. 2023, *ApJL*, 954, L4, doi: [10.3847/2041-8213/ace5a0](https://doi.org/10.3847/2041-8213/ace5a0)
- Kocevski, D. D., Finkelstein, S. L., Barro, G., et al. 2024, *arXiv e-prints*, arXiv:2404.03576, doi: [10.48550/arXiv.2404.03576](https://doi.org/10.48550/arXiv.2404.03576)
- Kokorev, V., Caputi, K. I., Greene, J. E., et al. 2024, *ApJ*, 968, 38, doi: [10.3847/1538-4357/ad4265](https://doi.org/10.3847/1538-4357/ad4265)
- Kouveliotou, C., Meegan, C. A., Fishman, G. J., et al. 1993, *ApJL*, 413, L101, doi: [10.1086/186969](https://doi.org/10.1086/186969)
- Krumholz, M., Thorsett, S. E., & Harrison, F. A. 1998, *ApJL*, 506, L81, doi: [10.1086/311657](https://doi.org/10.1086/311657)
- Labbé, I., van Dokkum, P., Nelson, E., et al. 2023, *Nature*, 616, 266, doi: [10.1038/s41586-023-05786-2](https://doi.org/10.1038/s41586-023-05786-2)
- Lamb, D. Q., & Reichart, D. E. 2000, *ApJ*, 536, 1, doi: [10.1086/308918](https://doi.org/10.1086/308918)
- Lan, G.-X., Wei, J.-J., Zeng, H.-D., Li, Y., & Wu, X.-F. 2021, *MNRAS*, 508, 52, doi: [10.1093/mnras/stab2508](https://doi.org/10.1093/mnras/stab2508)
- Lan, G.-X., Zeng, H.-D., Wei, J.-J., & Wu, X.-F. 2019, *MNRAS*, 488, 4607, doi: [10.1093/mnras/stz2011](https://doi.org/10.1093/mnras/stz2011)
- Langer, N., & Norman, C. A. 2006, *ApJL*, 638, L63, doi: [10.1086/500363](https://doi.org/10.1086/500363)
- Le, T., & Dermer, C. D. 2007, *ApJ*, 661, 394, doi: [10.1086/513460](https://doi.org/10.1086/513460)
- Levan, A. J., Jonker, P. G., Saccardi, A., et al. 2024, *arXiv e-prints*, arXiv:2404.16350, doi: [10.48550/arXiv.2404.16350](https://doi.org/10.48550/arXiv.2404.16350)

- Li, L.-X. 2008, *MNRAS*, 388, 1487, doi: [10.1111/j.1365-2966.2008.13488.x](https://doi.org/10.1111/j.1365-2966.2008.13488.x)
- Li, Z., Dekel, A., Sarkar, K. C., et al. 2023, arXiv e-prints, arXiv:2311.14662, doi: [10.48550/arXiv.2311.14662](https://doi.org/10.48550/arXiv.2311.14662)
- Liu, Y., Sun, H., Xu, D., et al. 2024, arXiv e-prints, arXiv:2404.16425, doi: [10.48550/arXiv.2404.16425](https://doi.org/10.48550/arXiv.2404.16425)
- Llamas Lanza, M., Godet, O., Arcier, B., et al. 2024, *A&A*, 685, A163, doi: [10.1051/0004-6361/202347966](https://doi.org/10.1051/0004-6361/202347966)
- Lloyd-Ronning, N., Hurtado, V. U., Aykutaalp, A., Johnson, J., & Ceccobello, C. 2020, *MNRAS*, 494, 4371, doi: [10.1093/mnras/staa1057](https://doi.org/10.1093/mnras/staa1057)
- Lloyd-Ronning, N. M., Fryer, C. L., & Ramirez-Ruiz, E. 2002, *ApJ*, 574, 554, doi: [10.1086/341059](https://doi.org/10.1086/341059)
- MacFadyen, A. I., & Woosley, S. E. 1999, *ApJ*, 524, 262, doi: [10.1086/307790](https://doi.org/10.1086/307790)
- Madau, P., & Dickinson, M. 2014, *ARA&A*, 52, 415, doi: [10.1146/annurev-astro-081811-125615](https://doi.org/10.1146/annurev-astro-081811-125615)
- Mao, S., & Mo, H. J. 1998, *A&A*, 339, L1, doi: [10.48550/arXiv.astro-ph/9808342](https://doi.org/10.48550/arXiv.astro-ph/9808342)
- Marchant, P., Langer, N., Podsiadlowski, P., Tauris, T. M., & Moriya, T. J. 2016, *A&A*, 588, A50, doi: [10.1051/0004-6361/201628133](https://doi.org/10.1051/0004-6361/201628133)
- Matsumoto, T., Nakauchi, D., Ioka, K., Heger, A., & Nakamura, T. 2015, *ApJ*, 810, 64, doi: [10.1088/0004-637X/810/1/64](https://doi.org/10.1088/0004-637X/810/1/64)
- Matsumoto, T., Nakauchi, D., Ioka, K., & Nakamura, T. 2016, *ApJ*, 823, 83, doi: [10.3847/0004-637X/823/2/83](https://doi.org/10.3847/0004-637X/823/2/83)
- Matthee, J., Naidu, R. P., Brammer, G., et al. 2024, *ApJ*, 963, 129, doi: [10.3847/1538-4357/ad2345](https://doi.org/10.3847/1538-4357/ad2345)
- McGuire, J. T. W., Tanvir, N. R., Levan, A. J., et al. 2016, *ApJ*, 825, 135, doi: [10.3847/0004-637X/825/2/135](https://doi.org/10.3847/0004-637X/825/2/135)
- McLeod, D. J., Donnan, C. T., McLure, R. J., et al. 2024, *MNRAS*, 527, 5004, doi: [10.1093/mnras/stad3471](https://doi.org/10.1093/mnras/stad3471)
- McQuinn, M., Lidz, A., Zaldarriaga, M., Hernquist, L., & Dutta, S. 2008, *MNRAS*, 388, 1101, doi: [10.1111/j.1365-2966.2008.13271.x](https://doi.org/10.1111/j.1365-2966.2008.13271.x)
- Menon, S. H., Lancaster, L., Burkhart, B., et al. 2024, *ApJL*, 967, L28, doi: [10.3847/2041-8213/ad462d](https://doi.org/10.3847/2041-8213/ad462d)
- Mészáros, P., & Rees, M. J. 2010, *ApJ*, 715, 967, doi: [10.1088/0004-637X/715/2/967](https://doi.org/10.1088/0004-637X/715/2/967)
- Miralda-Escudé, J. 1998, *ApJ*, 501, 15, doi: [10.1086/305799](https://doi.org/10.1086/305799)
- Nagakura, H., Suwa, Y., & Ioka, K. 2012, *ApJ*, 754, 85, doi: [10.1088/0004-637X/754/2/85](https://doi.org/10.1088/0004-637X/754/2/85)
- Naidu, R. P., Oesch, P. A., van Dokkum, P., et al. 2022, *ApJL*, 940, L14, doi: [10.3847/2041-8213/ac9b22](https://doi.org/10.3847/2041-8213/ac9b22)
- Nakane, M., Ouchi, M., Nakajima, K., et al. 2024, arXiv e-prints, arXiv:2407.14470, doi: [10.48550/arXiv.2407.14470](https://doi.org/10.48550/arXiv.2407.14470)
- Nakauchi, D., Suwa, Y., Sakamoto, T., Kashiyama, K., & Nakamura, T. 2012, *ApJ*, 759, 128, doi: [10.1088/0004-637X/759/2/128](https://doi.org/10.1088/0004-637X/759/2/128)
- Natarajan, P., Albanna, B., Hjorth, J., et al. 2005, *MNRAS*, 364, L8, doi: [10.1111/j.1745-3933.2005.00094.x](https://doi.org/10.1111/j.1745-3933.2005.00094.x)
- Palmerio, J. T., & Daigne, F. 2021, *A&A*, 649, A166, doi: [10.1051/0004-6361/202039929](https://doi.org/10.1051/0004-6361/202039929)
- Parashari, P., & Laha, R. 2023, *MNRAS*, 526, L63, doi: [10.1093/mnras/slzd107](https://doi.org/10.1093/mnras/slzd107)
- Patel, M., Warren, S. J., Mortlock, D. J., & Fynbo, J. P. U. 2010, *A&A*, 512, L3, doi: [10.1051/0004-6361/200913876](https://doi.org/10.1051/0004-6361/200913876)
- Pérez-González, P. G., Costantin, L., Langeroodi, D., et al. 2023, *ApJL*, 951, L1, doi: [10.3847/2041-8213/acd9d0](https://doi.org/10.3847/2041-8213/acd9d0)
- Pérez-González, P. G., Barro, G., Rieke, G. H., et al. 2024, *ApJ*, 968, 4, doi: [10.3847/1538-4357/ad38bb](https://doi.org/10.3847/1538-4357/ad38bb)
- Perley, D. A., Tanvir, N. R., Hjorth, J., et al. 2016, *ApJ*, 817, 8, doi: [10.3847/0004-637X/817/1/8](https://doi.org/10.3847/0004-637X/817/1/8)
- Pescalli, A., Ghirlanda, G., Salvaterra, R., et al. 2016, *A&A*, 587, A40, doi: [10.1051/0004-6361/201526760](https://doi.org/10.1051/0004-6361/201526760)
- Petrosian, V., Kitanidis, E., & Kocevski, D. 2015, *ApJ*, 806, 44, doi: [10.1088/0004-637X/806/1/44](https://doi.org/10.1088/0004-637X/806/1/44)
- Planck Collaboration, Aghanim, N., Akrami, Y., et al. 2020, *A&A*, 641, A6, doi: [10.1051/0004-6361/201833910](https://doi.org/10.1051/0004-6361/201833910)
- Porciani, C., & Madau, P. 2001, *ApJ*, 548, 522, doi: [10.1086/319027](https://doi.org/10.1086/319027)
- Preece, R. D., Briggs, M. S., Mallozzi, R. S., et al. 2000, *ApJS*, 126, 19, doi: [10.1086/313289](https://doi.org/10.1086/313289)
- Price, P. A., Cowie, L. L., Minezaki, T., et al. 2006, *ApJ*, 645, 851, doi: [10.1086/504414](https://doi.org/10.1086/504414)
- Punturo, M., Abernathy, M., Acernese, F., et al. 2010, *Classical and Quantum Gravity*, 27, 194002, doi: [10.1088/0264-9381/27/19/194002](https://doi.org/10.1088/0264-9381/27/19/194002)
- Qin, S.-F., Liang, E.-W., Lu, R.-J., Wei, J.-Y., & Zhang, S.-N. 2010, *MNRAS*, 406, 558, doi: [10.1111/j.1365-2966.2010.16691.x](https://doi.org/10.1111/j.1365-2966.2010.16691.x)
- Reitze, D., Adhikari, R. X., Ballmer, S., et al. 2019, in *Bulletin of the American Astronomical Society*, Vol. 51, 35, doi: [10.48550/arXiv.1907.04833](https://doi.org/10.48550/arXiv.1907.04833)
- Ricci, R., Troja, E., Yang, Y., et al. 2024, arXiv e-prints, arXiv:2407.18311, doi: [10.48550/arXiv.2407.18311](https://doi.org/10.48550/arXiv.2407.18311)
- Robertson, B., Johnson, B. D., Tacchella, S., et al. 2024, *ApJ*, 970, 31, doi: [10.3847/1538-4357/ad463d](https://doi.org/10.3847/1538-4357/ad463d)
- Robertson, B. E., & Ellis, R. S. 2012, *ApJ*, 744, 95, doi: [10.1088/0004-637X/744/2/95](https://doi.org/10.1088/0004-637X/744/2/95)
- Salpeter, E. E. 1955, *ApJ*, 121, 161, doi: [10.1086/145971](https://doi.org/10.1086/145971)
- Salvaterra, R. 2015, *Journal of High Energy Astrophysics*, 7, 35, doi: [10.1016/j.jheap.2015.03.001](https://doi.org/10.1016/j.jheap.2015.03.001)
- Salvaterra, R., & Chincarini, G. 2007, *ApJL*, 656, L49, doi: [10.1086/512606](https://doi.org/10.1086/512606)

- Salvaterra, R., Guidorzi, C., Campana, S., Chincarini, G., & Tagliaferri, G. 2009a, MNRAS, 396, 299, doi: [10.1111/j.1365-2966.2008.14343.x](https://doi.org/10.1111/j.1365-2966.2008.14343.x)
- Salvaterra, R., Della Valle, M., Campana, S., et al. 2009b, Nature, 461, 1258, doi: [10.1038/nature08445](https://doi.org/10.1038/nature08445)
- Salvaterra, R., Campana, S., Vergani, S. D., et al. 2012, ApJ, 749, 68, doi: [10.1088/0004-637X/749/1/68](https://doi.org/10.1088/0004-637X/749/1/68)
- Schechter, P. 1976, ApJ, 203, 297, doi: [10.1086/154079](https://doi.org/10.1086/154079)
- Sears, H., Chornock, R., Strader, J., et al. 2024, ApJ, 966, 133, doi: [10.3847/1538-4357/ad2e93](https://doi.org/10.3847/1538-4357/ad2e93)
- Steinhardt, C. L., Kokorev, V., Rusakov, V., Garcia, E., & Sneppen, A. 2023, ApJL, 951, L40, doi: [10.3847/2041-8213/acdef6](https://doi.org/10.3847/2041-8213/acdef6)
- Sun, H., Zhang, B., & Li, Z. 2015, ApJ, 812, 33, doi: [10.1088/0004-637X/812/1/33](https://doi.org/10.1088/0004-637X/812/1/33)
- Suwa, Y., & Ioka, K. 2011, ApJ, 726, 107, doi: [10.1088/0004-637X/726/2/107](https://doi.org/10.1088/0004-637X/726/2/107)
- Tanvir, N. R., Fox, D. B., Levan, A. J., et al. 2009, Nature, 461, 1254, doi: [10.1038/nature08459](https://doi.org/10.1038/nature08459)
- Tanvir, N. R., Levan, A. J., Fruchter, A. S., et al. 2012, ApJ, 754, 46, doi: [10.1088/0004-637X/754/1/46](https://doi.org/10.1088/0004-637X/754/1/46)
- Toma, K., Sakamoto, T., & Mészáros, P. 2011, ApJ, 731, 127, doi: [10.1088/0004-637X/731/2/127](https://doi.org/10.1088/0004-637X/731/2/127)
- Totani, T. 1997, ApJL, 486, L71, doi: [10.1086/310853](https://doi.org/10.1086/310853)
- Totani, T., Kawai, N., Kosugi, G., et al. 2006, PASJ, 58, 485, doi: [10.1093/pasj/58.3.485](https://doi.org/10.1093/pasj/58.3.485)
- Totani, T., Aoki, K., Hattori, T., et al. 2014, PASJ, 66, 63, doi: [10.1093/pasj/psu032](https://doi.org/10.1093/pasj/psu032)
- Tsuna, D., Nakazato, Y., & Hartwig, T. 2023, MNRAS, 526, 4801, doi: [10.1093/mnras/stad3043](https://doi.org/10.1093/mnras/stad3043)
- Virgili, F. J., Zhang, B., Nagamine, K., & Choi, J.-H. 2011, MNRAS, 417, 3025, doi: [10.1111/j.1365-2966.2011.19459.x](https://doi.org/10.1111/j.1365-2966.2011.19459.x)
- Wanderman, D., & Piran, T. 2010, MNRAS, 406, 1944, doi: [10.1111/j.1365-2966.2010.16787.x](https://doi.org/10.1111/j.1365-2966.2010.16787.x)
- Wang, F. Y. 2013, A&A, 556, A90, doi: [10.1051/0004-6361/201321623](https://doi.org/10.1051/0004-6361/201321623)
- Wang, F. Y., & Dai, Z. G. 2009, MNRAS, 400, L10, doi: [10.1111/j.1745-3933.2009.00751.x](https://doi.org/10.1111/j.1745-3933.2009.00751.x)
- Wei, J., Cordier, B., Antier, S., et al. 2016, arXiv e-prints, arXiv:1610.06892, doi: [10.48550/arXiv.1610.06892](https://doi.org/10.48550/arXiv.1610.06892)
- White, N. E. 2020, in Gamma-ray Bursts in the Gravitational Wave Era 2019, ed. T. Sakamoto, M. Serino, & S. Sugita, 51–53, doi: [10.48550/arXiv.2003.01592](https://doi.org/10.48550/arXiv.2003.01592)
- Wijers, R. A. M. J., Bloom, J. S., Bagla, J. S., & Natarajan, P. 1998, MNRAS, 294, L13, doi: [10.1046/j.1365-8711.1998.01328.x](https://doi.org/10.1046/j.1365-8711.1998.01328.x)
- Woosley, S. E. 1993, ApJ, 405, 273, doi: [10.1086/172359](https://doi.org/10.1086/172359)
- Wu, T. Y., & Fishbach, M. 2024, arXiv e-prints, arXiv:2408.04064, doi: [10.48550/arXiv.2408.04064](https://doi.org/10.48550/arXiv.2408.04064)
- Xiao, M., Oesch, P., Elbaz, D., et al. 2023, arXiv e-prints, arXiv:2309.02492, doi: [10.48550/arXiv.2309.02492](https://doi.org/10.48550/arXiv.2309.02492)
- Yin, Y.-H. I., Zhang, B.-B., Yang, J., et al. 2024, arXiv e-prints, arXiv:2407.10156, doi: [10.48550/arXiv.2407.10156](https://doi.org/10.48550/arXiv.2407.10156)
- Yonetoku, D., Murakami, T., Nakamura, T., et al. 2004, ApJ, 609, 935, doi: [10.1086/421285](https://doi.org/10.1086/421285)
- Yonetoku, D., Doi, A., Mihara, T., et al. 2024, in Space Telescopes and Instrumentation 2024: Ultraviolet to Gamma Ray, ed. J.-W. A. den Herder, S. Nikzad, & K. Nakazawa, Vol. 13093, International Society for Optics and Photonics (SPIE), 1309320, doi: [10.1117/12.3018571](https://doi.org/10.1117/12.3018571)
- Yuan, W., Zhang, C., Chen, Y., & Ling, Z. 2022, in Handbook of X-ray and Gamma-ray Astrophysics, 86, doi: [10.1007/978-981-16-4544-0_151-1](https://doi.org/10.1007/978-981-16-4544-0_151-1)
- Yüksel, H., Kistler, M. D., Beacom, J. F., & Hopkins, A. M. 2008, ApJL, 683, L5, doi: [10.1086/591449](https://doi.org/10.1086/591449)